International Core Journal of Engineering Volume 5 Issue 10, 2019
ISSN: 2414-1895 DOI: 10.6919/ICJE.201909_5(10).0007

Experimental study on wind load characteristics of double-sided spherical shell roof subjected to downburst

Liufeng Su

School of Civil Engineering and Architecture, Southwest University of Science and Technology, Sichuan Mianyang 621000, China

344107296@qq.com

Abstract

In order to study the roof wind pressure distribution characteristics of the double-sided spherical shell-type large-span roof structure under the flat terrain conditions under the action of the downburst, a double-sided spherical shell type large-span roof rigid scale model was fabricated based on the similarity criterion, and the impact jet was utilized. The device simulates the downburst wind field, and studies the influence of the change of the flow field position on the wind pressure distribution of the upper and lower roofs, the extreme position of the wind pressure and its numerical value. The test results show that with the increase of the radial distance under the flat working conditions, the windward surface of the roof gradually changes from positive pressure to negative pressure, and the negative pressure extreme value appears at the edge of the windward surface. The wind pressure on the lower roof wind gradually increases. Decrease, but always maintain a positive pressure. The position of the double-sided spherical shell roof model in the wind field has a great influence on the positive and negative wind pressure transition of the upper and lower roof, the position where the extreme wind pressure appears, and the numerical value of the wind pressure distribution. The closer the model is to the impact At the jet center, the vertical wind pressure is more obvious.

Keywords

Double-sided spherical shell roof; downbrust; wind tunnel test; wind pressure characteristic.

1. Introduction

As a novel structural system, the double-sided spherical shell roofing structure is more and more widely used with the rapid development of the economy, as shown in Figure 1. Large-span spatial structures are usually relatively low. In the atmospheric boundary layer, where the wind speed changes greatly and the turbulence is high, the flow and aerodynamic effects are very complicated. At present, the wind-resistance design of large-span structures is generally based on the wind field characteristics of the atmospheric boundary layer, but relevant studies have shown that the extreme wind speeds in many regional meteorological records are often the wind speed under the impact of the downburst [1]. The downburst is a common strong convection special weather, because of its high frequency, strong destructive power and strong suddenness [2], it has received great attention in the engineering community. The downburst wind field profile is very different from the common atmospheric boundary layer wind field profile. It is a strong wind load at a height of about 10m, and the instantaneous wind force can exceed 12, which has a strong destructive power to the local building structure in the area where it occurs. One of the causes of wind damage in many building structures around the world [3]. In the paper, wind tunnel test is carried out to study the distribution of wind

ISSN: 2414-1895 DOI: 10.6919/ICJE.201909_5(10).0007

pressure on the upper and lower surfaces of the double-sided spherical shell-type large-span structure on the flat terrain, and the influence of different radial distances on the wind pressure distribution on the upper and lower surfaces is preliminarily investigated. .

2. Impact jet model pressure test

2.1 Double-sided spherical shell roof model and measuring point arrangement

This test mainly studies the wind pressure distribution characteristics of the double-sided spherical shell type large-span roof model under the action of the impinging jet device, so the test adopts the rigid model. The scale of the double-sided spherical shell roof model is 1:1000, which is consistent with the impact jet device. Due to the characteristics of the curved surface of the model, 3D printing is used to ensure the accuracy of the model while making it have a certain rigidity and pressure measurement. The model is not affected by the vibration of the model, and the model dimensions are shown in Figure 5. The model measuring point arrangement is shown in Figure 1(b), with 193 measuring points on the upper surface and 95 measuring points on the lower surface, a total of 288 measuring points are arranged; the M-M' connecting line is the upper roof center line, L -L' is the centerline of the lower roof, and x is the distance from any point on the centerline to the edge of the windward side.

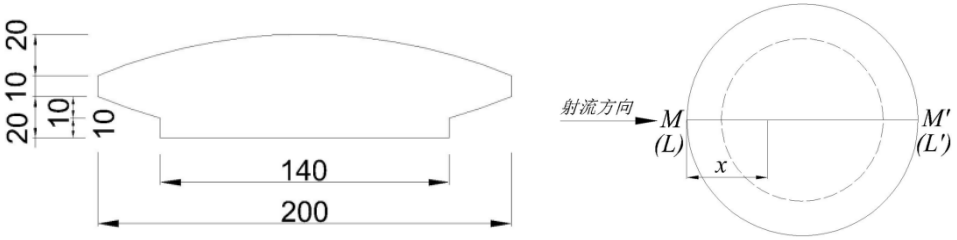

(a) Schematic diagram of the roof model

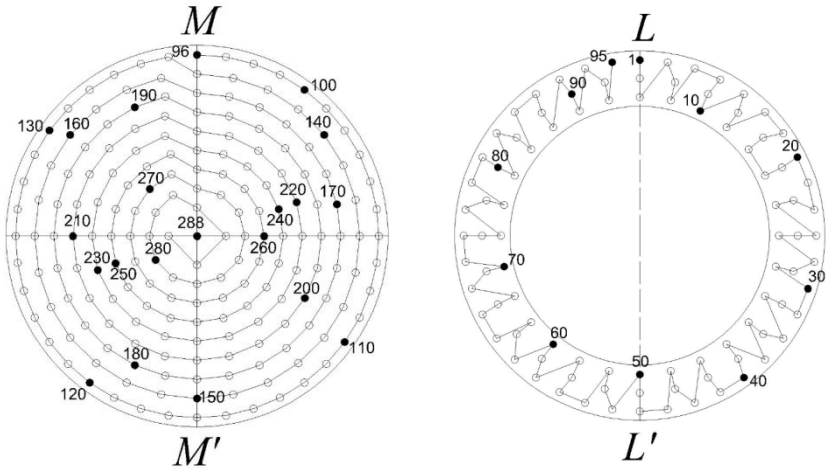

(b) Arrangement of the upper and lower roof points of the model

Figure 1. Schematic diagram of the double-sided spherical shell model and the arrangement of measuring points

In order to compare the wind pressure of the upper and lower roofs of the double-sided spherical shell large-span roof model on the flat and sloped land, the wind pressure coefficient Cp is used to express the relative wind pressure. The expression is

$$C_p = \frac{P}{0.5\rho v_r^{\ 2}} \tag{1}$$

ISSN: 2414-1895 DOI: 10.6919/ICJE.201909_5(10).0007

2.2 Leveling condition parameter setting

According to relevant research, the jet velocity and the jet diameter have little effect on the downburst wind field. Under normal circumstances, the jet velocity of the actual downburst is generally greater than or equal to the jet orifice diameter, so The parameters of the impinging jet device in this test were set to a fixed working condition, that is, the nozzle diameter D_{jet}=600 mm, the outflow velocity V_{jet}=10 m/s, the nozzle inclination angle θ_{jet}=0°, and the nozzle distance from the test plane height H_{jet}=2.0 D_{jet}. From the results of the previous wind field test, it is known that the horizontal wind speed reaches the maximum at r=1.0D_{jet}, and the double-sided spherical shell type has a large size. Therefore, when studying the effect of the double-sided spherical shell roof under the storm, The distance r from the center of the roof to the center of the jet is 0.75D_{jet}, 1.0D_{jet}, 1.25D_{jet}, 1.5D_{jet} and 2.0D_{jet}. In addition, considering the maximum vertical wind speed [x] directly below the jet surface, it is necessary to place the model at r=0.0D_{jet} directly below the jet surface to study the effect of vertical wind load on the roof. The specific location of the model placement is shown in Figure 2

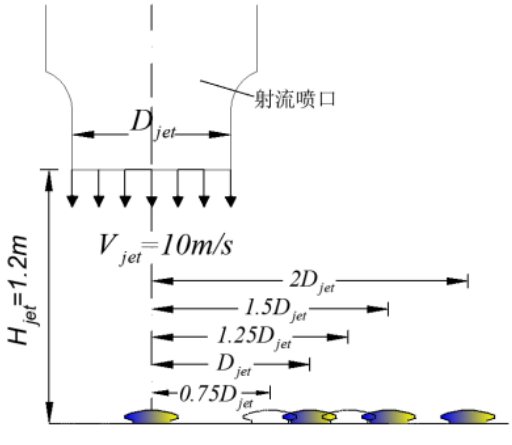

Figure 2.Schematic diagram of the position of the flat working condition model

2.2.1 The impact of the wind on the roof when the model is located directly below the downburst

The downburst has a distinct vertical wind speed component, which is greatly different from the atmospheric boundary layer wind field. If the double-sided spherical shell type large-span roof structure is just below the downburst, it will be subjected to a great vertical wind load. It can be seen from Fig.3 that when the model is placed directly below the jet device (r=0.00Djet), due to the direct action of the airflow, the roof on the model is subjected to a large vertical wind load, and the wind pressure on the roof is positive wind pressure. In the central region, the wind pressure value is close to 1.0, and the wind pressure on the outer side of the roof is slightly smaller than the central area; the roof wind pressure is also positive wind pressure under the model, and its value is slightly smaller than the upper surface, but the overall wind pressure distribution is not much different.

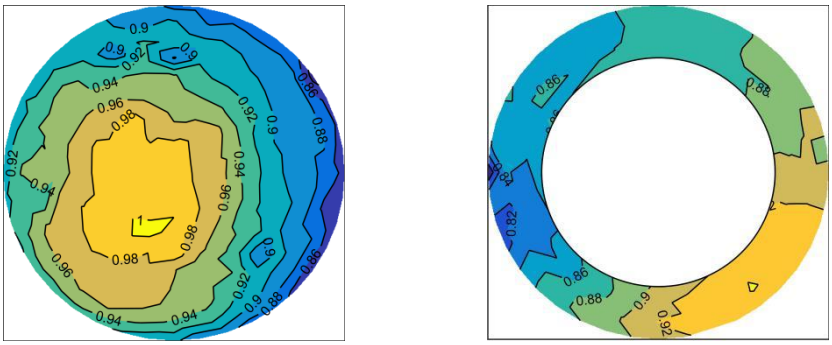

(a) Upper roof wind pressure distribution (b) Lower roof wind pressure distribution

Figure 3. Wind pressure distribution of the model roof when the nozzle is directly below

ISSN: 2414-1895 DOI: 10.6919/ICJE.201909_5(10).0007

2.2.2 The impact of the downburst on the roof when the model is at different radial distances

Figure 4 shows the wind pressure distribution on the upper surface under the action of the storm wind load under the working conditions of the flat ground. It can be seen from the figure that the contour of the wind pressure coefficient of each working condition is basically symmetrical about the roof center line M-M'. When the radial distance r=0.75Djet, the windward surface of the upper roof is positive wind pressure, and the maximum positive pressure value is about 0.7. The leeward surface is negative wind pressure, the maximum negative pressure value is about -0.3, and the absolute value of negative wind pressure is relatively small. As the radial distance r increases, the positive pressure zone on the roof gradually decreases, and the value decreases accordingly. Small, the negative pressure zone correspondingly increases, the positive pressure rapidly changes to negative pressure at the front edge of the windward side; when r=1.0D_{jet}, there is only a very small positive pressure zone on the windward side of the upper roof, the positive pressure value is about 0.1, facing the wind From the positive pressure maximal zone to the negative pressure zone, the wind pressure value changes from 0.7 to -0.3, and the maximum negative wind pressure value of the leeward surface also increases, which is about -0.5; when r=1.25D_{jet} The wind pressure on the upper roof becomes negative wind pressure, and the front end edge becomes the negative pressure maximum area, and the negative pressure value reaches -1.09; when the r=1.5D_{jet} is reached, as the radial distance continues to increase, The wind pressure distribution on the upper roof tends to be stable, and the negative pressure extreme value decreases due to the increase of the distance.

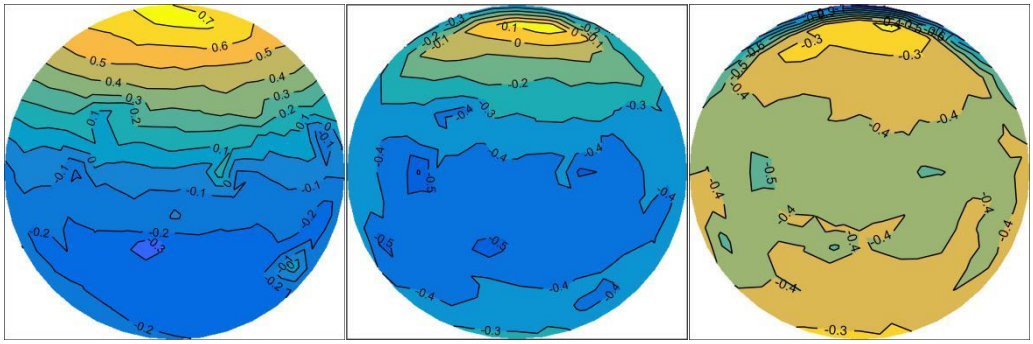

(a) r=0.75D_{jet} (b) r=1.00D_{jet} (c) r=1.25D_{jet}

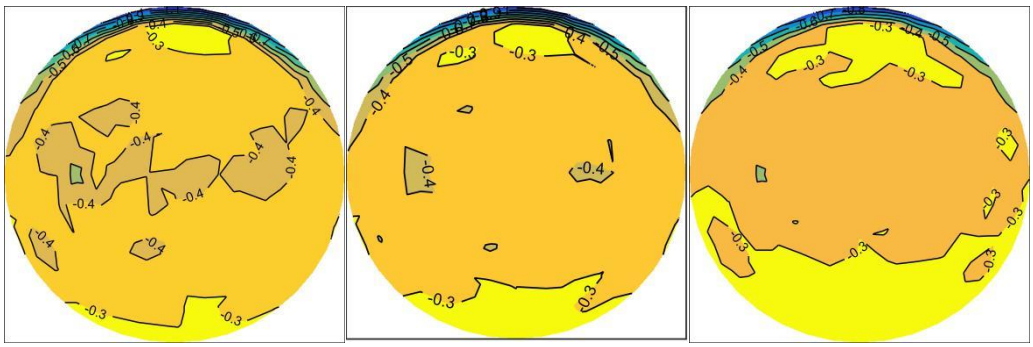

(d) r=1.50D_{jet} (e) r=1.75D_{jet} (f) r=2.00D_{jet}

Figure 4. Distribution of wind pressure on the roof of the model under various working conditions

Fig. 5 is a graph showing the wind pressure coefficient of the roof center line M-M' on the flat working condition model. As shown in the figure, when the radial distance r is less than 1.25D_{jet}, there is positive wind pressure on the windward surface of the roof on the model, and the positive wind pressure increases with the decrease of the radial distance r, and the wind pressure distribution on the upper surface is radial. The influence of distance is obvious; when the radial distance r is greater than 1.25D_{jet}, the wind pressure on the upper surface of the model is negative wind pressure, the wind pressure distribution tends to be stable, and the radial distance is no longer obvious for its wind pressure distribution; After the distance r reaches 1.00D_{jet}, the impact airflow separates at the

ISSN: 2414-1895 DOI: 10.6919/ICJE.201909_5(10).0007

edge of the windward side of the roof. At this time, a large negative pressure is generated at this point. When r=1.50D_{jet}, the negative wind pressure at the edge of the windward surface reaches a maximum value. It is -1.20, and then as the radial distance continues to increase, the negative wind pressure at the edge of the windward surface begins to decrease. When *x/L* reaches about 0.8, the wind pressure distribution on the leeward surface of the roof is basically the same. The wind pressure near the edge of the leeward surface is stable at around -0.3, and the radial distance has no significant effect on its negative pressure.

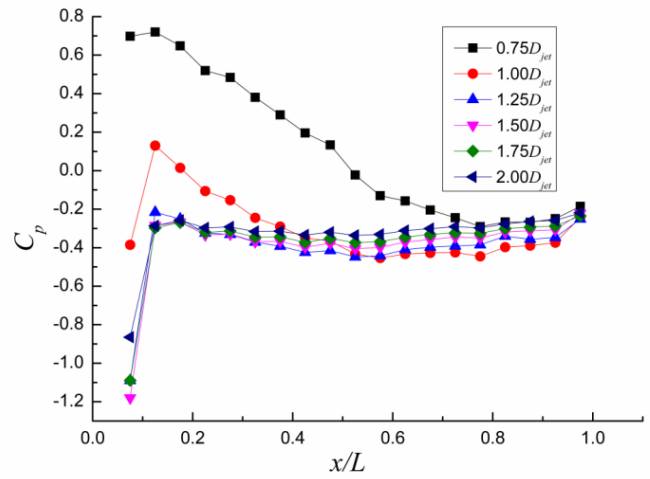

Figure 5. Curve of wind pressure coefficient of the upper roof center line with different radial distances r

Figure 6 shows the wind pressure distribution on the lower surface under the horizontal wind load of the downburst under various working conditions. It can be seen from the figure that the impact wind that propagates laterally along the surface forms a backflow after hitting the lower cylindrical surface of the model, causing wind pressure on the windward side of the lower roof near the lower cylindrical surface of the model, so the windward surface of the lower roof is positive wind pressure; The negative pressure zone appears on the left and right sides. The reason is that the lateral impact wind forms a shunt at the lower cylinder of the model, and the wind speed on the left and right sides increases, causing the negative pressure value to increase. With the increase of the radial distance, the positive wind pressure on the windward side of the lower roof gradually decreases, but it always maintains a positive pressure; the leeward surface of the lower roof is negative pressure, and the negative pressure value and the distribution area increase with the radial distance. Has not changed much.

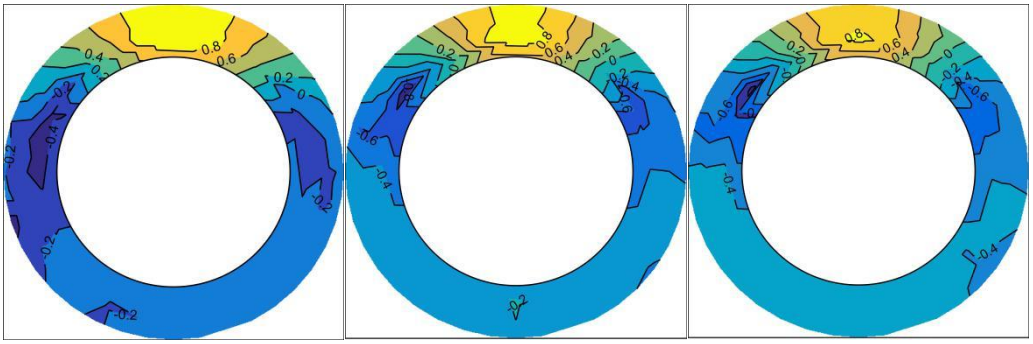

(a) r=0.75D_{jet} (b) r=1.00D_{jet} (c) r=1.25D_{jet}

ISSN: 2414-1895 DOI: 10.6919/ICJE.201909_5(10).0007

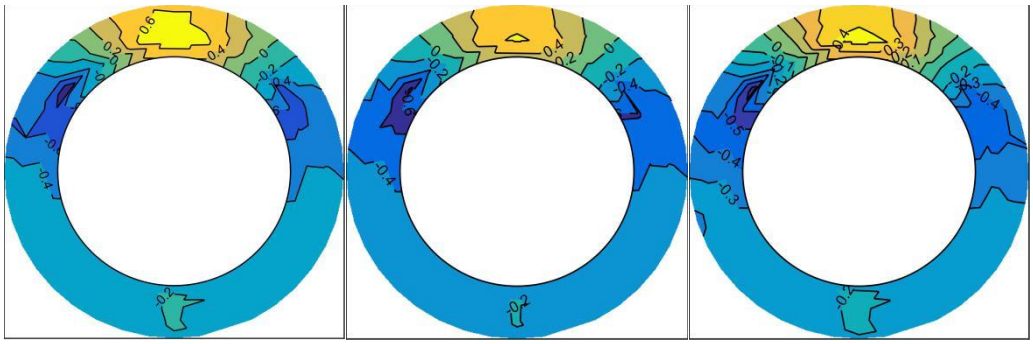

(d) r=1.50D_{jet} (e) r=1.75D_{jet} (f) r=2.00D_{jet}

Figure 6. Distribution of roof wind pressure under the model under various working conditions

Figure 7 is a plot of the wind pressure coefficient of the roof centerline L-L' under the flat condition model. As shown in the figure, the wind pressure on the windward side of the roof is positive wind pressure, and the pressure is steadily decreasing as the radial distance of the model increases from the nozzle; the model is at the same radial distance and its windward side is positive. The wind pressure increases with the increase of x/L. The reason is that the impact wind that propagates laterally along the surface hits the lower cylindrical surface of the model and forms a reflow, which causes wind pressure on the windward side of the lower roof near the lower cylindrical surface of the model. The wind pressure on the windward side of the roof is closer to the vertical cylindrical surface. Under the model, the wind pressure on the leeward surface of the roof is negative wind pressure, and the negative pressure value is about -0.15 when r=0.75D_{jet}; when the radial distance r reaches 1.00D_{jet}, the negative wind pressure on the lower roof leeward tends to be stable. It is about -0.2; as the radial distance continues to increase, the wind pressure value does not change much, and is about -0.2.

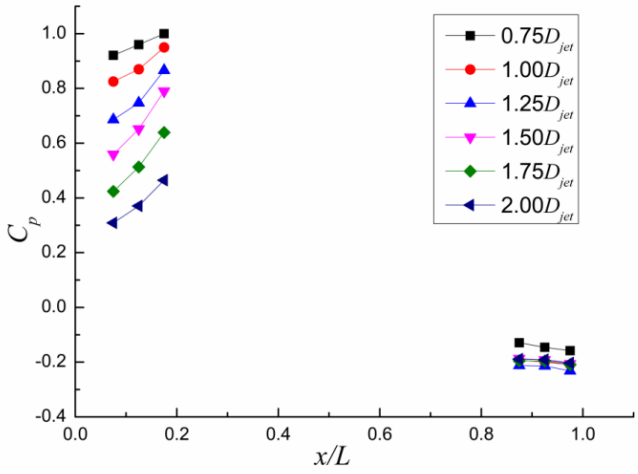

Figure 7. Curve of wind pressure coefficient of the center line of the roof under different radial distances r

3. Conclusion

A rigid scale model was made for the double-sided spherical shell-type large-span roof, and the wind tunnel test was carried out under the impact of the downburst. A systematic experimental study on the effect of the roof model on the downburst in the flat terrain was carried out. Research indicates:

(1)When the model roof is under the downburst, the roof is mainly affected by the vertical wind load. The wind pressure coefficient of the upper roof is more than 1 and the wind pressure distribution has the largest central area. The wind pressure coefficient is smaller near the edge of the roof; the wind pressure coefficient of the lower roof is not changed much, and its value is slightly smaller than the upper roof.

ISSN: 2414-1895 DOI: 10.6919/ICJE.201909_5(10).0007

(2)Under the condition of flat terrain, the wind pressure distribution on the windward surface of the roof is greatly affected by the topographic factors; the wind pressure distribution on the leeward surface of the model is not affected by the topography, and the wind pressure distribution on the centerline is basically the same under all working conditions; The trend is that the positive wind pressure on the windward side of the roof increases with the decrease of the distance of the jet center, while the absolute value of the negative wind pressure on the leeward side decreases accordingly, reflecting the vertical wind speed effect of the impact wind field.

References

[1] Holmes J D. Modeling of extreme thunderstorm winds for wind loading of structures and risk sssessment ［C］// Proceedings of 10th International Conference on Wind Engineering,Wind Engineering into 21st Century. Rotterdam,Denmark: Balkema,1999: 1409-1415.

[2] Letchford C W,Mans C M,Chay M T. Thunderstorms-their importance in wind engineering: a case for the next generation wind tunnel ［J］. Journal of Wind Engineering and Industrial Aerodynamics,2002,90(12 /13 /14 /15) : 1415-1433.

[3] CHOI E C C,TANURDJAJA A. Extreme wind studiesin Singapore: an area with mixed weather system ［J］. Journal of Wind Engineering ＆ Industrial Aerodynamics,2002,90(12) : 1611-1630.

[4] Chen L , Letchford C W.Multi-scale correlation analysis oftwo lateral profiles of ful-l scale dow nburst w ind speeds[J] .Journal of Wind Engineering and Industrial Aerody namics,2006 , 94(9):675-696 .

[5] Hjelmfelt MR. Structure and life circle of micro burst out flows observed in Colorado[J] .J.Appl.Meteorol, 1988, 27(8):900 -927.

[6] MASON M S,WOOD G S, FLETCHER D F. Impinging jet simulation of stationary downburst flow over topography ［J］. Wind and Structures,2007,10 (5) : 437-462.

[7] MASON M S,WOOD G S,FLETCHER D F.Influence of tilt and surface roughness on the outflow wind field of an impinging jet ［J］. Wind and Structures,2009,12 (3) : 179-204.

[8] MASON M S, WOOD G S,FLETCHE R D F. Numerical simulation of downburst winds ［J］. Journal of Wind Engineering and Industrial Aerodynamics, 2009,97(11 /12) : 523-539.

[9] MASON M S. Numerical investigation of the influence of topography on simulated downburst wind fields ［J］. Journal of Wind Engineering and Industrial Aerodynamics,2010,98(1) : 21-33.